HIGH POWER VACUUM ELECTRIC ARC STUDY AND TECHNOLOGICAL APPLICATIONS

D. Pavelescu[1], V. Braic[2], F. Gherendi[3], Mariana Braic[2], C.Nitu[1],
M. Balaceanu[2], G. Dumitrescu[4], Gabriela Pavelescu[2], Smaranda Nitu[1], Paula Anghelita[4]

[1] *"POLITEHNICA" University of Bucharest, 313, Spl. Independentei, Bucharest, ROMANIA*
[2] *National Institute for Optoelectronics, P.O.Box. MG 05, Bucharest -Magurele, ROMANIA*
[3] *National Institute for Lasers, Plasma and Radiation Physics, P.O.Box. MG 06, Bucharest-Magurele, ROMANIA*
[4] *Research and Development Institute for Electrical Industry , 313, Spl. Unirii, Bucharest ROMANIA*

Abstract – The present paper deals with the problem of the TMF interruption systems breaking capability concerning vacuum circuit breakers. The main goal is a better understanding of the physical phenomena taking place during the interruption process, for high currents, corresponding to short-circuit regime in the electrical networks. The arc appearance and its behaviour were explored with a dedicated optical system. An example of spatial and temporal distribution of the arc light intensity is presented. Specific peculiarities of the optical spectra recorded in the proximity of the short circuit current zero (c.z.) moments are reported. Different current interruption situations are correlated with plasma spectral diagnosis. On this basis the authors try to define a set of plasma parameters which are critical in the studied interruption processes.

I. INTRODUCTION

The modern power apparatus using vacuum interrupters are world-wide used in the electrical networks. A tendency to extend their application to the high voltage and low voltage domains is very clear, because of their obvious advantages.

The main problem of the vacuum circuit breakers, in the short-circuit regime, is the breaking capability value. It is known that the interrupting current depends basically on the electrode diameter. During the high current evolution, when the current value exceeds 10kA, the arc column has the tendency to concentrate and the arc forms an anode spot. Due to its very high temperature, the anode spot produces an intense vaporization of the contact material and can produce specific craters in the electrode surface. As a result, the current interruption is severely impeded and the life-time of the contact parts is reduced. In order to avoid such effects, there are known two main technical solutions:

? The axial magnetic field (AMF) technique

Using an AMF, the arc is maintained in the diffuse mode, even in the case of high currents. Consequently, the column concentrating effect diminishes and the energy density distribution over the butt contact pieces is quasi-uniform. After the c.z. moment, the interruption process is facilitated by the fact that the high frequency oscillation of the post-arc current is severely dumped by an AMF [1].

? The transverse magnetic field (TMF) technique

In the case of the TMF solution, the arc column becomes concentrated during the high current interruption process. In order to avoid its negative effects, the vacuum arc is rapidly moved over the contact surfaces.

By magnetic driven motion of the column [2], the arc energy is homogeneously distributed on the contact surface, avoiding local over heating and facilitating the successful current interruption. There are known two main designs: spiral type and cup-shaped contacts.

In this paper, the preliminary results obtained by the electrical and optical investigation of the rotating arc plasma, in a TMF cup-shaped interruption system, are presented. In the authors' opinion, such structure can provide the technical solution for the future low voltage vacuum circuit breakers.

II. EXPERIMENTAL SET-UP

In order to study the vacuum electric arc behaviour, a specific facility that reproduces exactly the short-circuit regime in the low voltage distribution network, was used.

The experimental setup is similar with a direct test scheme that includes a power transformer supplied from the medium voltage network [3]. The transformer provides 1140V; 960V and 660V in its secondary windings. A synchronous contactor initiates the prospective current that can have different degrees of asymmetries. The prospective current can reach 50kA at 960V. A digitised control system provides a testing current with duration of 5 - 6 half waves.

The vacuum interrupter model is a detachable stainless steel vessel with glass windows for the arc observation. A mechanical synchronous system, based on Thomson effect, produces the opening movement of the contact parts, with a variable velocity, (0.8 - 1.5 m/s) in order to initiate the vacuum arc. The opening moment can be fixed by a digital timer and allows reproducing the vacuum arc in similar physical conditions. The c.z. moment interruption is identical with the real network situation, producing the transient recovery voltage and post arc current.

The vacuum chamber contains a cup-shaped contact (Cu75 Cr25), with 12 slots at an angle of 60°. The diameter of the contact (inner and outer diameters are 50 mm and 75mm respectively) is correlated with the rated current. The maximum gap between the contact parts is 8 mm.

The arc evolution was studied by an optical multi-channel detection system with maximum 8 channels, mounted on two orthogonal directions, enabling the recording of the arc light intensity using a dedicated digital acquisition system [4]. The length of the collimator (680 mm) and the width of the slits (2 mm), in which the optical fibers are introduced, provide for each observation channel a spatial resolution of 3 mm.

Simultaneously with the optical detection, time resolved spectroscopy was performed with an Acton SP750 spectrograph and intensified CCD camera. A 16 gates burst of 500 μs width and 1ms period was used to trigger the CCD camera, in order to have the required time resolution while recording the arc emission in a single shot.

III. OPTICAL AND SPECTROSCOPIC INVESTIGATION

Arc appearance

The optical detection scheme is presented in Fig.1

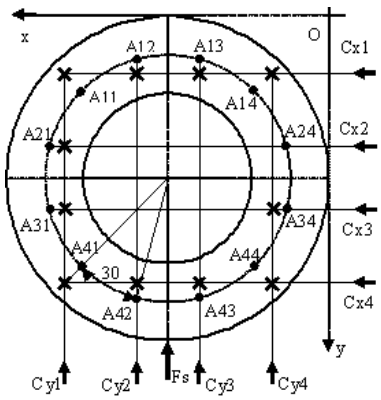

Fig.1 Optical detection scheme

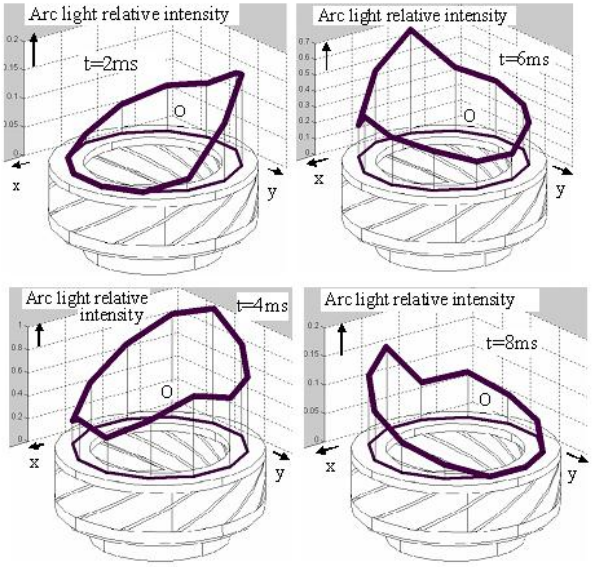

Fig.2. Arc appearance at different moments in current arc evolution (t=2ms, t=4ms); t=6ms; t=8ms) resulted from the optical determinations.

The position of the 8 observing channels permits to measure the light intensity emitted by the arc in points placed at 30° on the contact circumference. There are 4 channels (Cxi, with i=1÷4) recording the arc light intensity along the Ox direction and other 4 channels (Cyj, with j=1÷4) recording the arc light intensity along the Oy direction.

The 8 signals are proportional with the linear integral of the light emission intensity along the chosen direction. The results are used assuming the following hypotheses:

Arc movement

Fig. 2 shows the arc relative light intensity distributed over the contact rim, corresponding to a successful interruption at a current of 9 kA peak value. In this case the arc is in the diffuse mode. The origin of the time in the process is established at the very current onset. The drawing arc has a duration of 9 ms and the arc column presents a tendency to rotate, accordingly with the Laplace force.

In the case of currents corresponding to the short circuit regime (i.e.100 kA) the arc column is constricted by the Pinch effect. In our experiments, the vacuum arc is concentrated and rotate over the contact rim for currents exceeding 12 kA.

A configuration with two optical channels to record the arc light in two orthogonal positions was used, in order to evaluate the velocity of the high current arc.

Fig.3 presents two typical oscilograms for 17kA and 26 kA current values. The Ch1 presents the interrupted current, Ch2-CCD trigger signal, Ch3 and Ch4 - optical fibers.

The maximum of the light intensity of the two optical fibers corresponds to the arc passage in front of the Ox and Oy measuring channel. The time elapsed between the maximum values of the two optical records corresponds to the arc movement on a quarter of the contact circumference. In the case of a multiple half wave interruption it is noticeable that the arc velocity in the first current half wave is almost constant (e.g. for currents of 17kA and 26 kA

the velocity is about 15m/s). For the following current half waves the measured velocity could rich 120 m/s depending on the current intensity [2].

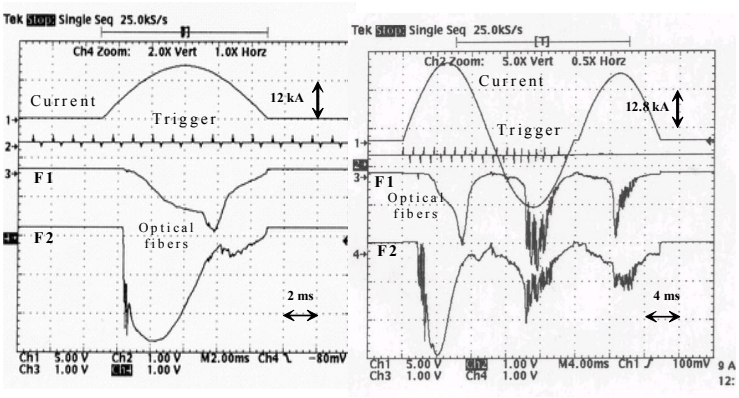

Fig. 3 . Typical oscillograms at 17 kA and 26 kA:
Ch1-current, Ch2 –trigger CCD; Ch3- optical fiber F1, Ch4- optical fiber F2

Spectroscopic investigation

For the spectroscopical study of the vacuum arc interruption, the TMF system was fit to the limit of its breaking capability. Consequently the contact opening speed was fixed at lowest value (0.8 m/s). In this situation, the vacuum interruption process had the following aspects:

1- successful (interruption at first c.z. moment)
2- partial unsuccessful interruption (at second c.z. moment)
3- partial unsuccessful interruption (at the third c.z. moment)
4- total unsuccessful (interruption is not possible)

For currents up to 17 kA successful and partial unsuccessful interruption (1-2) occurred. In the case of 26 kA, only partial and total unsuccessful interruptions were observed (2-3-4).

These aspects made possible the comparison between different series of spectra measured in the case of identical short circuit conditions, but with different evolution of the interruption process. It is worth to note that in the partial unsuccessful interruption (3), the second c.z. moment always presents an interruption tendency, with a current pause of almost 500 μs. Comparing the spectra measured near different c.z. moments, specific peculiarities concerning the interruption process could be derived. The arc plasma parameters exhibit specific evolution behaviour depending on different macroscopic interruption situations.

In fig. 4 an example of spectra recorded in the case of partial and total unsuccessful interruption is presented. For both situations, the light intensity exhibits higher values in the first half period and a reduced intensity in the second one, suggesting that the arc column emits plasma jets under the influence of the Laplace force.

For determining the plasma parameters, a Monte-Carlo simulation-fit code SimSpec [5] was further developed. The simulation code assumes Boltzmann-like plasma with a volume emissivity of the transition between *u-l* levels given by:

$$I_{ul} = \frac{h \cdot c}{\lambda} \cdot \frac{g_u \cdot A_{ul}}{U_z(T)} \cdot n_z \cdot \exp\left(-\frac{E_u}{k \cdot T}\right) \quad (1)$$

with A_{ul} the transition probability, E_u the upper level energy of the transition, g_u the statistical weight, T the excitation temperature, n_z the species density. $U_z(T)$ is the partition function for the specie *z,* which depends on the ionization

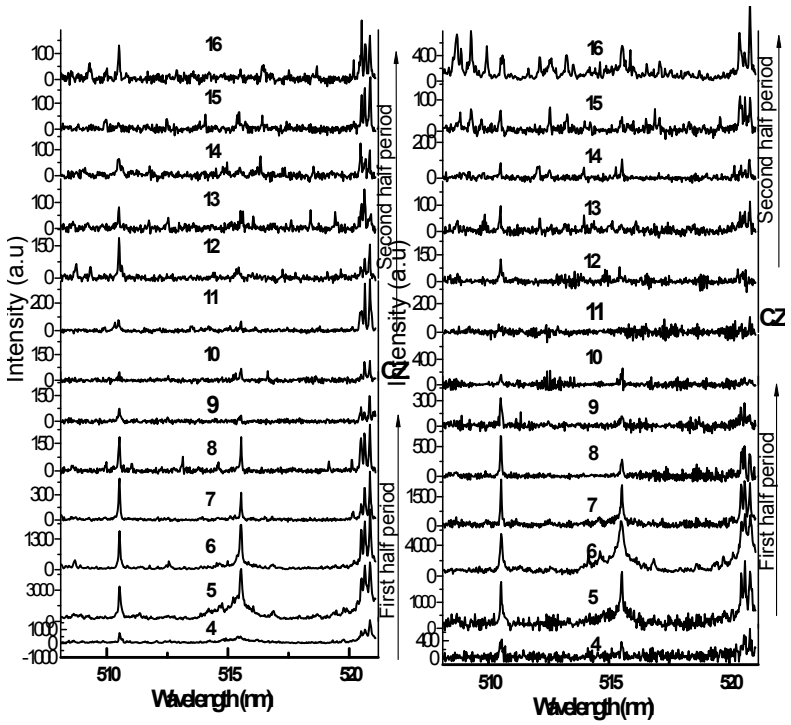

(a) (b)

Fig.4 Example of spectra corresponding to the partially (a) and total (b) unsuccessful interruption (the gate number -800μs width- is indicated on each spectra)

potential lowering ΔE :

$$U_z(T) = \sum_{u=1}^{u=u\max} g_u \cdot \exp\left(-\frac{E_u}{k \cdot T}\right) \tag{2}$$

u_{max} is the last excited energy level with an energy lower than the ionisation potential ($E_{umax}<E_i-\Delta E$).

In order to compute the partition functions and the line profiles, sequences inspired from the COSSAM [6] code were included into the SimSpec source program. With these changes, SimSpec can simulate large Stark and/or Van der Waals broadenings. The new code sequences made possible to introduce the electron density and temperature as simulation parameters

. The program determines the best fit for the measured spectrum using simulated densities and temperatures for all species and also for electrons. In order to resolve the superposed lines emitted by different species (which is the case for almost all Cu and Cr lines) the simulation is performed on parallel threads.

The simulated spectra compose a global spectrum, which is compared with the measured one. The simulation stops if the global error between the measured and simulated data reaches a minimum in the limits of given convergence parameters.

Table 1 Plasma temperatures and species abundances (17 kA) before first c.z.

Species	Successful interruption		Unsuccessful interruption	
	Temperature [K]	Abundance [cm^{-3}]	Temperature [K]	Abundance [cm^{-3}]
Cu I	19528	$2.7*10^{13}$	10000	$6.4*10^{16}$
Cr I	16481	$5.2*10^{16}$	15400	$4.1*10^{15}$
Cu II	9162	$6.6*10^{22}$	19873	$8.8*10^{16}$
Cr II	11220	$4*10^{19}$	15256	10^{17}

Table 2: Electron density and temperature (17 kA) before first c.z.

	Successful interruption	Unsuccessful interruption
n_e [m^{-3}]	$9*10^{17}$	$6.5*10^{17}$
T_e [K]	10800	17672

Plasma parameters for 17 kA arc current in the case of successful and partial unsuccessful interruption were determined. The temperature of various species, the electron density and temperature before the c.z. are presented in Tables 1and 2. It can be seen that the Cr species are in thermal equilibrium, most probably because the low energy excited levels of Cr can be closer to local thermodinamical equilibrium (LTE) than the higher energy levels of Cu ionized species.

Generally, Cu species are never in equilibrium for the vacuum arc [5]. In table 1 a new parameter was introduced – the so called "species abundance", corresponding to the total number of emitting particles found in the optical fiber line of sight. The new parameter was introduced as a replacement for the species densities, because in the experiment it is not possible to observe the spatial distribution of all species in the arc plasma and thus calculate their densities.

In the case of unsuccessful interruption higher temperatures for Cu ions compared to Cr species. In the same time, Cu ions are hotter than Cu atoms. In the case of successful interruption, a higher electrons density and a lower electrons temperature were obtained, suggesting that higher arc conductivity leads to lower dissipation in plasma, favourizing a faster cooling of the arc in the moment of c.z. Compared to the neutrals, high ionic "abundances" at low temperatures (especially CuII) suggests that they are cooled by expansion in the whole volume seen by the optical fiber.

The analysis of 26 kA arc current unsuccessful interruption, before and after c.z. is presented in tables 3-4. Comparing to 17 kA interruption, it is noticeable that Cr species are still in thermal equilibrium while Cu remains in non-LTE after c.z. For obvious reasons, the higher the arc energy, the higher the temperatures and electron densities. It can be mentioned that the electron temperature is closer to the ionized species temperature, suggesting that the partial thermodinamical equilibrium (PLTE) condition is fulfilled for the Cu species.

After the arc reignition, CuII ion number increases, but the temperature is almost the same, proving that no cooling-by-expansion occurs even after the c.z. In the case of 17 kA current unsuccessful interruption (Table 1), it can be noticed that the abundance of CuI is higher than

CrI, while CuII temperature is higher than Cr II temperature.

Table 3 Temperatures and species abundances
(26 kA arc current unsuccessful interruption)

	Before c.z		After c.z.	
	Temperature [K]	Abundance [m^{-3}]	Temperature [K]	Abundance [m^{-3}]
Cu I	5700	$3.6*10^{16}$	6300	$2.4*10^{17}$
Cr I	22600	$1.6*10^{13}$	25900	$1.5*10^{13}$
Cu II	22500	10^{14}	25500	$4.4*10^{14}$
Cr II	21000	$5*10^{14}$	21800	$1.4*10^{15}$

Table 4: Electron parameters for 26 kA arc current unsuccessful interruption

	Before c.z	After c.z.
n_e [m^{-3}]	$6.8*10^{20}$	$2.5 – 4*10^{20}$
T_e [K]	10000 – 15000	15000 – 19000

V. CONCLUSIONS

Using the optical system the arc light intensity was measured and the arc column, spatial and temporal evolution, was recorded. A tendency to rotate of the vacuum arc in the TMF contacts was present, even for the currents under 10 kA, when the arc is in diffuse mode.

In the case of high currents, when the arc is concentrated, the arc velocity estimated in the first current half wave is smaller that in the next half waves. The spectroscopic study shows a plasma "memory effect" of the vacuum arc. Events which are happening in the first half-period, systematically influence the events in the next half-period of the current.

Comparing the successful and unsuccessful interruptions, in the successful one the most important factor seems to be the cooling of CuII. It appears that the responsible for unsuccessful interruption may be the high temperature of Cu II on the background of a high abundance of Cu I. Also, the CrII temperature is higher in the case of unsuccessful interruption while its abundance is lower.

This means that the arc reignition occurs rather on a thin discharge channel than in the whole inter-electrode space. In conclusion, an intense constricted arc already exists in the very first moment of the reignition. An axial magnetic field can prevent constricted arc formation, by creating helical paths of the charged particles in the discharge channel.

The most important conclusion is that the reignition in low voltage vacuum arc is not a dielectric breakdown; plasma is already there, with the tendency to recombine and to expand, being still enough conductive to be re-heated when the current increases again. This derived behaviour would also explain the different ionisation degree observed in the successive half-periods.

Acknowledgements:
The work was accomplished with the support of NATO SfP 974083 – LOVARC Project and the NATO CORINT National Program.

REFERENCES

[1] D.Pavelescu, S.Nitu, G.Dumitrescu, P.Anghelita, "Post-arc Current in Low Voltage Vacuum Circuit Breaker: Measurements and Physical Peculiarities", *IEEE Trans. Plasma Sci.,* vol. 31, nr. 5, pp. 869-876, 2003.

[2] E. Dullni, E. Schade, W. Shang, "Vacuum arc driven by cross-magnetic fields (RMF)", *Proc. ISDEIV XXth, Tours, France,* 2002, pp.60-66.

[3] D.Pavelescu, V.Trusca, S.Nitu, "Installation and equipment for the research of the electrical switching arc in advanced vacuum*", Proc. ISDEIV XVIIth, Berkeley, California*, 1996, pp. 305-309.

[4] V.Zoita, D.Pavelescu, G.Sandolache, N.Georgescu, "Time and space resolved analysis of the visible radiation from a vacuum circuit breaker discharge", *Proc. ISDEIV XVIIth, Berkeley, California*, 1996, pp.310-313.

[5] F.Gherendi, "Etude de la transition d'un regime diffus a un regime anodique du plasma du disjuncteur sous vide. Spectroscopie, imagerie et autres diagnostics", PhD Thesis, University of Orleans, France (2001)

[6] COSSAM: COdice per la Sintesi Spettrale nelle Atmosfere Magnetiche, Vienna University, Astrophysics Laboratory, online documentation and ADA language source code at http://fedelma.astro.univie.ac.at/web/cossam_public